Meiosis-specific prophase-like pathway controls cleavage-independent release of cohesin by Wapl

Kiran Challa[1], Ghanim Fajish V[1], Miki Shinohara[1, 5], Franz Klein[2], Susan M. Gasser[3] and Akira Shinohara[1, *]

[1]Institute for Protein Research, Graduate School of Science, Osaka University, Suita, Osaka 565-0871, Japan
[2]Max F. Perutz Laboratories, University of Vienna, A-1030 Vienna, Austria
[3]Friedrich Miescher Institute for Biomedical Research, 4058 Basel, Switzerland

[5]Present address: Kindai University, School of Agriculture

Running title: Cleavage-independent release of meiotic cohesin

Key words: Cohesin, meiosis, prophase pathway, Rec8

*To whom correspondence should be addressed:
Akira Shinohara
Institute for Protein Research, Osaka University,
3-2 Yamadaoka, Suita, Osaka 565-0871 JAPAN
Phone: 81-6-6879-8624
FAX: 81-6-6879-8626
E-mail: ashino@protein.osaka-u.ac.jp
ORCID: 0000-0003-4207-8247

Summary

Sister chromatid cohesion on chromosome arms is essential for the segregation of homologous chromosomes during meiosis I while it is dispensable for sister chromatid separation during mitosis. It was assumed that, unlike the situation in mitosis, chromosome arms retain cohesion prior to onset of anaphase-I. Here we show that approximately half of the meiosis-specific cohesin, including the kleisin Rec8, is released from meiotic chromosomes during late prophase-I. This release is independent of cleavage by separase and requires the cohesin regulator, Wapl (Rad61/Wpl1 in yeast), and Polo-like kinase (PLK). Meiosis-specific phosphorylation of Rad61/Wpl1 and Rec8 by PLK and the Dbf4-dependent Cdc7 kinase (DDK) promote this release. This process is similar to the vertebrate “prophase” pathway for cohesin release during G2 phase and pro-metaphase. In yeast, meiotic cohesin release coincides with PLK-dependent compaction of chromosomes in late meiotic prophase-I. We suggest that yeast uses this highly regulated cleavage-independent pathway to remove cohesin during late prophase-I in order to facilitate chromosome morphogenesis.

Introduction

Meiosis gives rise to haploid gametes from diploid germ cells. During meiosis, a single round of DNA replication is followed by two consecutive chromosome segregations, meiosis I and II, which reduce the number of chromosomes by half (Marston, 2014). Homologous chromosomes are separated during meiosis I (MI), and sister chromatids are segregated during meiosis II (MII). Sister chromatid cohesion (SCC) acts as physical connection between the segregating chromosomes and provides resistance to pulling forces by microtubules. SCC along chromosome arms and at the kinetochore plays a critical role in chromosome segregation during MI and MII, respectively. For accurate chromosome segregation at MI, SCC along chromosome arms, and chiasmata, which are the cytological manifestation of crossovers, are essential for generating tension between the homologous chromosomes.

SCC is mediated by a protein complex, called cohesin, that is able to embrace two sister chromatids in a ring-shaped structure (Gruber et al., 2003). The core subunits of cohesin are composed of two structure-maintenance complex (SMC) ATPases, Smc1 and Smc3, as well as a kleisin subunit, Scc1/Mcd1/Rad21 (hereafter, Scc1 for simplicity). Smc1 and Smc3, both of which consist of a rod-like structure with an ATPase head, form a heterodimeric ring, which entraps two DNA molecules. Scc1 bridges between the Smc1 and Smc3 ATPase head domains to lock the ring.

Chromosomal localization of cohesin is highly dynamic, and is strictly regulated. During the G1 phase, the loading of cohesin is mediated by the Scc2-Scc4 loader complex. This process itself is not sufficient for SCC formation, however, SCC establishment occurs in S phase, during which the Eco1 acetyl-transferase catalyzes Smc3 acetylation. SCC is thereafter maintained until the onset of anaphase, when Scc1 is cleaved by the protease separase. This results in the release of the two entrapped sister chromatids. Separase activity is regulated by the protein securin, which binds to separase to inhibit its function. This process is closely monitored during the spindle-assembly checkpoint (SAC) to ensure that each chromosome is properly attached to the spindle apparatus prior to separation. SAC negatively controls the protein ubiquitination machinery, the anaphase-promoting complex/cyclosome (APC/C), whose activation is

essential for entry into anaphase. Activation of APC/C requires the Cdc20 and APC/C-Cdc20 targets securin for destruction which in turn enables the separation of sister chromatids. Thus, the activity of Cdc20 plays a critical role in Scc1 cleavage, and consequently, the transition from metaphase to anaphase.

Cohesin dynamics are regulated by other cohesin-interacting proteins in yeasts and vertebrates, such as Scc3, Pds5 and Rad61/Wpl1 (Wapl), with vertebrates also having a Wapl antagonist, sororin (Nishiyama et al., 2010). Wapl, together with Pds5, negatively regulates the binding of cohesin to chromatin (Gandhi et al., 2006; Kueng et al., 2006). Wapl-regulated cohesin dissociation is independent of Scc1 cleavage, allowing entrapped DNAs to be released from the cohesin ring by the opening the “exit gate” at the interphase between Smc3 and Scc1 (Chan et al., 2012; Gruber et al., 2006). Eco1-mediated Smc3 acetylation locks the gate (Rowland et al., 2009; Sutani et al., 2009) and sororin interacts with the cohesin complex to suppress Wapl activity (Nishiyama et al., 2010).

In vertebrate cells during late G2 or pro-metaphase, cohesin is removed from the majority of chromosome arms by a Scc1-cleavage-independent pathway (Haarhuis et al., 2014). This so-called “prophase pathway” for cohesin removal is triggered by the phosphorylation of sororin and Scc3 by polo-like kinase (PLK), aurora kinase, and cyclin-dependent kinase (CDK) (Nishiyama et al., 2010; Nishiyama et al., 2013). Phosphorylated sororin is inactive, and can no longer suppress Wapl activity. On the other hand, at kinetochores, the phosphorylation that triggers the prophase pathway is blocked by the action of Shugoshin, a protein that recruits a phosphatase, PP2A (Marston, 2015). PP2A is believed to dephosphoryate proteins involved in the prophase pathway, such as sororin. Interestingly, sororin is not present in lower eukaryotes such as budding yeast, and the prophase pathway of cohesin removal is absent in yeast mitosis (Lopez-Serra et al., 2013).

Cohesin also plays an essential role in chromosome segregation during meiosis (Marston, 2014). During meiosis, the kleisin Scc1 is replaced with its meiosis-specific counterpart, Rec8 (and also Rad21L in mammals) (Ishiguro et al., 2011; Klein et al., 1999; Lee and Hirano, 2011). The Rec8-cohesin complex is also involved in various chromosomal events such as homologous recombination and chromosome motion in the meiotic prophase-I (Trelles-Sticken et al., 2005;

Yoon et al., 2016). Cohesin is a major component of the chromosome axis, which contains two sister chromatids organized into multiple chromatin loops (Klein et al., 1999). During the pachytene, homologous chromosomes pair with each other, and synapse along chromosome axes to form a unique meiosis-specific chromosome structure, the synaptonemal complex (SC) (Loidl, 2016). The SC together with chromosome axes then dismantles to form a chiasma during diplotene and diakinesis/early metaphase-I. At the onset of anaphase-I, APC/C-Cdc20 induces securin degradation, which activates separase to allow cleavage of Rec8. Phosphorylation of Rec8 by three kinases, PLK, Dbf4-dependent Cdc7 kinase (DDK), and Casein kinase 1 (CK1) promotes this cleavage (Brar et al., 2006; Katis et al., 2010). Upon the onset of anaphase-I, the phosphorylation and cleavage of Rec8 is restricted to chromosome arms, while Rec8 at the kinetochores is protected by Shugoshin (Kitajima et al., 2004). It has been shown that Shugoshin blocks phosphorylation of Rec8 at the kinetochores by recruiting PP2A (Kitajima et al., 2006; Riedel et al., 2006). Protection of SCC at the kinetochores is essential for proper sister chromatids segregation at MII.

The disassembly of the chromosome axis and release a cohesin during meiotic prophase-I is poorly described. In budding yeast, late prophase-I stages such as diplotene and diakinesis are very short-lived, and are less well defined in terms of chromosome structure, than those in other organisms. Previously, immuno-staining showed a decreased intensity of Rec8-cohesin signal on meiotic chromosomes during late prophase-I, suggesting that Rec8 is released (Yu and Koshland, 2005). Here, we revisited this observation and found that in late prophase-I of budding yeast, approximately half of the full-length of Rec8 molecules are released from meiotic chromosomes. The Rec8 release is independent of cleavage by separase. This vertebrate “prophase-like” removal of cohesin in meiotic prophase-I is mediated by meiosis-specific phosphorylation of Rec8 as well as phosphorylation of Rad61/Wpl1 by DDK and PLK. Moreover, this process is coupled to changes in chromosome morphogenesis and chromosome compaction. We propose that cleavage-independent release of cohesin is a key regulator of meiotic chromosome function in late prophase-I.

Results

Rec8 shows dynamic localization during late prophase-I

Here we study the dynamics of axis proteins during late prophase-I. Because late-prophase I is a very short-lived stage in budding yeast meiosis (e.g. Fig. 1G; ~1.5 h from mid-pachytene and post-meiosis I in wild-type cells), we arrested cells prior to the onset of anaphase I using a meiosis-specific depletion mutant of *CDC20*, *cdc20mn* (meiotic null), which compromises activation of the anaphase promoting complex/cyclosome (APC/C). We then analysed the localization of chromosome axis proteins in this *cdc20mn* (meiotic null) mutant (Lee and Amon, 2003), over a meiotic time course. The staining of a central component of the SC, Zip1 (Sym et al., 1993), allowed us to classify stages of prophase-I as follows: I, dotty staining; II, short-line staining; III, long-line staining. Category III corresponds to pachytene, during which chromosome synapsis occurs. Following pachytene, the SC dismantles, resulting in the re-appearance of dotty Zip1 staining (class-I), some of which co-localizes with kinetochores (see below) (Gladstone et al., 2009). Disassembly of Zip1 was also found to correlate with dissociation of chromosome axis proteins such as Red1 (Fig. 1, A and B)(Rockmill and Roeder, 1988).

We observed long lines of Zip1 staining peaks at 5 h in *cdc20mn* mutants, followed by the appearance of Zip1 dots after 6 h (Fig. 1, A and B). When localization of Rec8 was analyzed in pachytene, Rec8 shows linear staining that co-localized with Zip1-lines (Fig. 1A). Following the pachytene stage, chromosome spreads with Zip1 dots (i.e. at 6 h) started to exhibit altered Rec8 staining associated with dotty staining (Fig. 1A). This indicated that the remodeling of cohesin localization takes place at or after SC disassembly. Altered Rec8 staining in the *cdc20mn* mutants accumulated for up to 8 h. The appearance of altered Rec8 staining occurred concomitantly with disassembly of SCs into Zip1-dots (Fig. 1B). To further characterize the disassembly status of the axes, we also examined Rec8-Red1 localization at later time points; chromosomal Red1 signals diminish with a conversion from long lines to short lines/dots when altered Rec8 staining is observed (Fig. 1, A and B). This result further confirmed that Rec8 remodeling occurs at or after disassembly of chromosome axis.

We then used super-resolution microscopy to analyze Rec8-cohesin localization on meiotic chromosomes at high resolution. A structural illumination microscope (SIM) was used to determine Rec8 localization in *cdc20mn* and *ndt80*, which arrests at the pachytene stage (Xu et al., 1995)(Fig. 1D). At 5 h, both strains showed two parallel lines of Rec8, which corresponded to two axes of full length SCs (Fig. 1D). More importantly, by SIM the two Rec8 lines do not show a uniform staining, but rather a beads-on-string-like staining was observed. This suggested non-continuous localization of Rec8-cohesin along the chromosome axis. Kinetochore visualization by staining of Ctf19, a centromere protein, revealed that each SC showed a single focus of Ctf19, indicating tight fusion of all four sister kinetochores. Two Rec8 lines were fused around the Ctf19 focal point, suggesting a unique axial structure at peri-centromeric regions with respect to Rec8-cohesin localization. In the *ndt80* mutant, these two Rec8 lines are maintained beyond 6 h. On the other hand, differential staining patterns were observed between 5 h and 8 h in *cdc20mn* mutants; the two clear parallel lines visible at 5 h disappear at 8h, where discrete focus or short-line staining of Rec8 dominate. This is consistent with the observations made by conventional fluorescent microscopy described above. At later time points in *cdc20mn* mutants, a Ctf19 focus at kinetochores is often flanked by two distinct Rec8 signals (Fig. 1D, see inset).

A previous study reported that the signal intensity of HA-tagged Rec8 was diminished during late prophase-I in *cdc20mn* as well as in wild type cells (Yu and Koshland, 2005). However, they did not observe the altered Rec8 staining at late stages and instead a uniform staining of reduced intensity was seen. This may be due to differences in the antibodies used. In the previous study, the localization of HA-tagged Rec8 was examined using an anti-HA antibody. In our study, localization of non-tagged Rec8 was examined using two independent anti-Rec8 antisera. We quantified Rec8 signals on chromosomal spreads, and also found reduced Rec8 signal at 8 h (61.9±7.6%) as compared with that at 5 h in *cdc20mn* mutants (Fig. 1C). This was supported by quantification of Rec8 signal in our SIM images (Fig. 1E). While epitope masking might also explain the decreased Rec8 signal, our results suggest that Rec8 dissociates from chromosomes during late prophase-I. Given that the decrease in Rec8 intensity was observed in *CDC20*

depletion cells arrested at meta/anaphase transition, Rec8 remodeling appeared to be independent of separase-mediated cleavage.

Because *CDC20* depletion may affect Rec8 localization during prolonged arrest, we confirmed Rec8 remodeling at late prophase-I by performing Rec8 and Red1 co-staining in a wild-type meiosis (Fig. 1, F and G). We examined spreads at 5 and 6 h when ~90% cells are still in prophase-I, classifying these into Red1-positive and -negative spreads, which corresponds with pachytene/zygotene and diplotene/prometaphase-I, respectively. We then checked the staining pattern of Rec8 and its intensity. As seen in *CDC20* depletion, the Red1-positive spreads showed linear Rec8 staining (Fig. 1F). On the other hand, Red1-negative spreads contained altered Rec8 signals. This staining was different from that at anaphase-I spreads, which shows two separated Rec8 foci with centromere clustering (Fig. 1F). Intensity measurements confirmed that Red1-negative spreads had reduced Rec8 signal (56.1±11.0% [n=20]) compared to Red1-positive spreads (100±15.1%; Fig. 1H). Thus, Rec8 remodeling occurs in late prophase-I in normal wild-type meiosis as well.

To make sure that Rec8 depletion is independent of its cleavage, the localization of a Rec8 mutant protein, Rec8-N, which is resistant to cleavage by separase, was also investigated (Buonomo et al., 2000). The *REC8-N* mutant strain showed normal prophase I progression, but is completely blocked at the metaphase/anaphase-I transition because Rec8-N is resistant to separase cleavage (Buonomo et al., 2000). Similar to the *cdc20mn* mutant, at late prophase-I, the *REC8-N* mutant exhibited altered Rec8 staining with reduced intensity (60±15.7%), while linear staining was observed at 5 h (Fig. 1, I and J). A previous study reported that the temperature-sensitive separase-deficient mutant, *esp1-1*, also showed a decrease in Rec8 intensity at late prophase-I at a restricted temperature (Yu and Koshland, 2005). Together, all observations support the hypothesis that Rec8 localization is remodeled and possibly released in late meiotic prophase-I in an independent way of Rec8 cleavage.

Rec8 dissociates from meiotic chromosomes at late prophase-I

To check whether Rec8-cohesin is indeed released from meiotic chromosomes in

cdc20mn mutants, we fractionated cell/nuclear lysates to separate the chromatin insoluble and soluble fractions. Chromatin insoluble fractions contained proteins tightly bound to chromosomes, such as histones. At 5 h, most of full-length Rec8 proteins were recovered in the insoluble fraction containing histone H2B in both *ndt80* and *cdc20mn* mutants (Fig. 2A and Fig. S1A). This argues that Rec8, and thus cohesin complex, is tightly bound to DNAs and/or chromatin. Rec8 is also chromatin-bound at 8 h in *ndt80* cells. On the other hand, a large proportion of Rec8 protein (69.0±18.9%) was recovered in the soluble fraction at 8 h in the *cdc20mn* mutant, while the remaining Rec8 protein was in the insoluble fraction (Fig. 2, A and B). Interestingly, the soluble Rec8 migrated more slowly on the gel than the insoluble Rec8. It has been shown that slow-migrating Rec8 is highly phosphorylated (Brar et al., 2006; Katis et al., 2010). Rec8 is a target of Dbf4-dependent Cdc7 kinase (DDK), Polo-like kinase (Cdc5), and casein kinase 1 (Hrr25). Its phosphorylation is believed to promote Rec8 cleavage by the separase, Esp1 (Brar et al., 2006; Katis et al., 2010). Our results suggested that, alternatively or in addition to cleavage, Rec8 phosphorylation triggers cohesin dissociation at late prophase-I.

We next checked the status of Smc3 acetylation at K112 and K113 during meiosis by chromatin fractionation (Chan et al., 2012). Acetylation of Smc3 occurs during DNA replication in order to facilitate the establishment of SCC. In *cdc20mn* mutants, most of the acetylated Smc3 was found in the chromatin-bound fractions at 5 h. This further confirmed that SCC formation is mediated by Smc3 acetylation in prophase-I. At 8 h, 51.6% of acetylated Smc3 was recovered in the unbound fraction (Fig. 2, A and C, and Fig. S1A). This showed that not only Rec8, but also acetylated Smc3, a core component of the cohesion complex, is released from the chromatin in late meiotic prophase-I.

To test the separase-sensitivity of the chromatin-bound Rec8 fraction during late prophase-I, we artificially induced expression of the separase, Esp1, in prophase-I under Cdc20 depletion conditions (*cdc20-mn*). Esp1 expression is driven by the *CUP1* promoter and copper was added at 3 and 5 h to induce Esp1 during prophase-I (Yoon et al., 2016). As above, Rec8 staining was reduced on chromatin at 8 h without Esp1 induction. Following Esp1 induction, a large number of Rec8 foci/lines disappeared, leaving only a few Rec8 foci per

chromosome (Fig. 2D). Indeed, the signal intensity of Rec8 dropped to 17.7±6.7% upon Esp1 induction, while at 5 h without Esp1 induction the Rec8 signal was reduced to 50.0±21.7% (Fig. 2E). This demonstrated that most of Rec8 on chromatin during late prophase-I in *cdc20mn* cells remains sensitive to separase. Similar results were obtained when copper was added at 3 h. Finally, the sensitivity of Rec8 to Esp1 was confirmed by chromatin fractionation (Fig. 2, F and G, and Fig. S1B). After 3 h of separase induction (8 h), the amount of full length Rec8 on chromatin was reduced to 26.2±10.8% (versus approximately 47.1±16.2% without Esp1 induction). The cleaved Rec8 products were too unstable to detect without a *ubr1* mutation which protects the product from degradation (Buonomo et al., 2000). Separase-resistant Rec8 foci often co-localize with the centromere marker Ctf19 (Fig. 2D). This confirms that kinetochores in late-prophase-I are able to protect Rec8 cohesin from cleavage by separase, while the arm-bound Rec8 appears more sensitive.

Rec8 phosphorylation is associated with dissociation of Rec8 at late prophase-I

To characterize the phosphorylation status of Rec8 during late prophase-I, we used two phospho-specific antibodies; anti-Rec8-pS179 (PLK site) and anti-Rec8-pS521 (DDK site; kindly gifted by A. Amon, MIT) (Attner et al., 2013; Brar et al., 2006). Probing chromatin fractions revealed that Rec8-pS179-specific signals were very few at 5 h, but increased at 8 h in whole cell lysates from the *cdc20mn* mutant. The signals were nearly undetectable in *cdc5mn cdc20mn* mutants, illustrating dependence on Cdc5 (Fig. 3, A and B). Importantly, at 8 h, the Rec8-pS179 signal was recovered primarily in soluble fraction. This indicated that Cdc5-dependent S179 phosphorylation is associated with Rec8 release from meiotic chromatin. We were unable to detect the Rec8-pS179 signal on spreads. This may either indicate that the Rec8-pS179 signal was removed from spreads, or that the Rec8-pS179 antibody is too weak to detect signal on spreads.

We stained meiotic chromosome spreads with anti-Rec8-pS521 antibody (Fig. 3C) (Brar et al., 2006), and, similar to Rec8 staining result, Rec8-pS521 shows a linear signal at 5 h in the *cdc20mn*. However, unlike Rec8, some of Rec8-pS521 (target of DDK) foci are brighter than other foci or lines, suggesting

local enhancement of S521 phosphorylation. Importantly, Rec8-pS521-specific signal on spreads was reduced at 8 h, leaving several bright foci. This loss of Rec8 signal depends on Cdc5 kinase since *cdc5mn cdc20mn* maintained high levels of Rec8-pS521 on chromosomes at the late time points (Fig. 3, C and D). Quantification revealed that Rec8-pS521-specific signal was even more strongly reduced than the global Rec8 signal (28.9±20% versus 56.8±18.6%). This is consistent with a model where by DDK triggers or contributes to cohesin release through Rec8 phosphorylation.

Taken together, the above results showed that Rec8-cohesin dissociates from meiotic chromosomes during late-prophase-I independent of separase activation. This suggests the presence of a cleavage-independent pathway for cohesin release that correlates with Rec8 phosphorylation. This is very similar to phosphorylation-dependent cohesin release in vertebrate pro-metaphase, the so-called mitotic “prophase pathway” (Haarhuis et al., 2014).

Rec8 phosphorylation is required for efficient dissociation of Rec8 at late prophase-I

To examine the role of Rec8 phosphorylation in cohesin release during late prophase-I, we localized phosphorylation-deficient Rec8 mutant proteins, Rec8-17A and -29A on meiotic spreads (Brar et al., 2009; Brar et al., 2006). We introduced *rec8-17A* and *-29A* mutations (Fig. S2A) into the *cdc20mn* background. The Rec8-17A still can be phosphorylated and shows a band shift, while Rec8-29A does not (Fig. S2B). We performed the same Rec8 localization studies and Rec8 staining was defined as linear or altered as above, which corresponding to the pachytene stage and late (early) prophase-I, respectively. Both Rec8-17A and -29A proteins showed a linear staining on meiotic chromosomes like the wild-type Rec8 protein (Fig. 4, A and B, Fig. S2C). In *rec8-17A* mutants, the appearance of altered Rec8 staining at late time points was slightly delayed as compared with the control (Fig. S2D). *rec8-29A* mutants, on the other hand, showed a strong delay in the appearance of an altered Rec8 staining pattern, and of the subsequent dissociation of cohesin (Fig. 4F). This was confirmed by intensity measurements (Fig. 4G and Fig. S2E). The *rec8-29A* mutant retained 78±25% of its Rec8 signal at 12 h when compared with the level

at 6 h. However, it is possible that the significant delay we observed for Rec8 release of this mutant in late prophase-I is due to defects early events such as the processing of meiotic recombination intermediates (Brar et al., 2009). Therefore, we also determined localization of Rec8-29A mutant proteins in chromosome spreads that lacked Red1 signals, those that correspond to late prophase-I. The change in Red1 staining showed a delay in late prophase-I in the *rec8-29A* mutant (Fig. 4, A and B). Delay in SC disassembly was observed also in the mutant (Fig. 4, C and D). Importantly, we found that 67.4% (n=68) of Red1-negative nuclei showed linear Rec8 staining in the *rec8-29A cdc20mn* mutant, a value that was only 5.17±0.75% (n=76) in *cdc20mn* cells. It is thus likely that Rec8 phosphorylation promotes the dissociation of Rec8 in late prophase-I as well as facilitating cohesin relies steps in meiosis.

Cdc5 is indispensable for cleavage-independent Rec8 dissociation from meiotic chromosomes

During the vertebrate mitotic “prophase pathway” for cohesin release is strongly dependent on Polo-like kinase (PLK) (Haarhuis et al., 2014). Therefore, we wondered whether Cdc5, the budding yeast PLK, also regulates this release through phosphorylation of Rec8 as previously suggested (Yu and Koshland, 2005). We depleted Cdc5 during meiosis in the absence of Cdc20 (*cdc5mn cdc20mn)*. Indeed, Cdc5 depletion greatly reduced the appearance of dotty Rec8 staining, and preserved Rec8 intensity at later time points, such as at 8 h (Fig. 3, E, F and G). This was supported by chromatin fractionation (Fig. 3, A and B). At 8 h, approximately half of Rec8 was released from chromatin in *cdc20mn* cells, and the release was not seen at 8 h in *cdc5mn cdc20mn* mutants (80±16% at 8 h relative to 5 h). In the absence of Cdc5, the mobility of Rec8 was rarely shifted up (Fig. 3A). Therefore, we conclude that Cdc5/PLK is critical for cleavage-independent removal of Rec8 in late meiotic prophase-I, possibly through the phosphorylation of Rec8.

A previous study showed that ectopic expression of Cdc5 is sufficient for exit from the mid-pachytene stage in *ndt80* mutants. This is triggered by resolution of recombination intermediates into products, as well as the disassembly of SC (without entry into meiosis I) (Clyne et al., 2003). We next

asked whether Cdc5 is sufficient for Rec8 chromatin dissociation by expressing Cdc5 ectopically during an *ndt80*Δ arrest. Expression of Cdc5 was induced by the addition of estradiol into the *CDC5-in ndt80* strain (Fig. 5C). In concert with Zip1-disassembly, Cdc5 induction led to the formation of altered Rec8 staining and thus cohesin release (Fig. 5, A and B). This process was dependent on the kinase activity of Cdc5, as kinase-dead *CDC5kd* (*CDC5-N209A*) mutants did not induce remodeling of the Rec8-containing structure during pachytene. Our data, argue that Cdc5 is both necessary and sufficient for cohesion release in mid-pachytene.

Rad61/Wpl1, the Wapl ortholog in yeast, regulates cohesin release during late-prophase-I

In the budding yeast, cohesin association in the mitotic G1 phase is inhibited by a Wapl ortholog, Rad61/Wpl1 (Lopez-Serra et al., 2013). The anti-cohesin activity of Rad61/Wpl1 is counteracted by Eco1-dependent acetylation of Smc3 (Rowland et al., 2009; Sutani et al., 2009) and no prophase-like pathway has been reported for mitotic G2 phase in budding yeast mitosis (Lopez-Serra et al., 2013). In mammalian cells, on the other hand, a vertebrate-specific protein, sororin, counteracts Wapl activity (Nishiyama et al., 2010). The fact that the budding yeast does not possess a sororin ortholog prompted us to examine the role of Rad61/Wpl1 in cohesin release during meiosis. Indeed, our previous report showed that in the *rad61/wpl1* mutant, the disassembly of Rec8 is much slower than the other axis component, Red1, whose disassembly is tightly correlated with Rec8 in wild-type (Challa et al., 2016). This suggested an uncoupling of disassembly steps for the two axis components during late prophase-I in *rad61/wpl1* mutants. Localization of Rec8 was examined in *cdc20mn* mutants lacking *RAD61/WPL1* (Fig. 6, A and B). As compared with *cdc20-mn*, *rad61/wpl1 cdc20mn* cells showed prolonged persistence of Rec8 lines at very late time points. Even at 14 h, 32.1±3% *rad61/wpl1* cells retained full linear Rec8 staining (Fig. 6, A and C). Indeed, the signal intensity of Rec8 was unchanged between 5 and 8 h in the absence of Rad61/Wpl1 (Fig. 6B). This suggests a key role of Rad61/Wpl1 in cohesin release in the G2 phase of yeast meiosis.

We investigated the expression of Rad61-Flag during meiosis by western blot, and found that Rad61 exhibits multiple bands upshifted during meiosis (Fig. 6D). Similar to Rec8, Rad61 expression disappears after 8 h. In addition to the two bands observed during pre-sporulation at 0 h, at least two major meiosis-specific forms of Rad61 were observed; one that started to appear at 3 h, and a second that appeared at 5 h. The slowly migrating forms of Rad61 disappeared at 8 h and were far less abundant relative to early time points. The appearance of two meiotic-specific forms of Rad61 protein, as well as its disappearance resembles Rec8, which also showed two major phosphorylated species in addition to the unmodified one (Brar et al., 2006; Katis et al., 2010). It seemed likely that Rad61 band shifts were due to phosphorylation, and since Rec8 phosphorylation is catalyzed by three kinases, DDK, PLK, and CK1(Brar et al., 2006; Katis et al., 2010), we checked the effects of these kinases on Rad61 modification. When the kinase activity of analog-sensitive Cdc7 (Cdc7-as) was suppressed by its inhibitor, PP1, band shifts of both Rec8 and Rad61 were greatly diminished in meiosis (Fig. 6E). After washing out PP1, the band shifts reappeared. These indicated that band shifts of Rad61 are dependent on Cdc7 (DDK) kinase activity.

We also checked the depletion of Cdc5 and found that the upper band shifts of both Rad61 and Rec8 at late time points (5 and 6 h) were nearly abolished in the *cdc5-mn* cells (Fig. 6F). These results showed that, like Rec8, the Rad61-band shift requires both DDK and PLK activities. Rad61 phosphorylation is independent of meiotic recombination and DSB formation, since *spo11-Y135F* mutants displayed normal Rad61 and Rec8 band shifts (Fig. S3F). On the other hand, Rec8 is essential for the PLK(Cdc5)-dependent secondary band shift of Rad61, although not the DDK-dependent one (Fig. 6H). This is consistent with the fact that Rec8 directly binds to Cdc5 kinase (Katis et al., 2010).

Based on the sequence information of Rad61 (Montagnoli et al., 2006), we mapped putative DDK sites in the N-terminal non-conserved region of Rad61, which is outside of a conserved WAPL domain (Fig. S3A). These sites were as follows: T13, S25, S69, S70, T95, S96, and S97. Various substitution combinations were generated for these putative sites: *rad61-T13A, S25A-FLAG*, *rad61-S69A, S70A-FLAG*, *rad61-T95A, S96A, S97A-FLAG*, *rad61-T13A, S25A,*

T95A, S69A, S70A, S96A, and S97A-FLAG (hereafter, *rad61-7A*) and we found that meiosis-specific band shifts of Rad61 were compromised in the *rad61-S69A, S70A-FLAG* and *rad61-7A* mutants but not in the *rad61-T13A, S25A-FLAG* and *rad61-T95A, S96A, S97A-FLAG* strains (Fig. 6G and Fig. S3E). We raised an antibody against a Rad61 peptide containing phospho-S69 and phospho-S70 sites and used it to detect phosphorylation-specific bands of Rad61. Western blotting using Rad61 phospho-specific antibody clearly revealed two meiosis-specific bands, which were absent in mitosis (Fig. 6G, right panels).

The *rad61-7A* mutant exhibited spore viability comparable to wild-type cells (Fig. S3, C and D), and entry into meiosis I was only delayed one hour (Fig. S3B), suggesting that Rad61 phosphorylation plays a minor role in early prophase-I. We then investigated the effect of the *rad61-7A* mutation on Rec8 dissociation at late prophase-I in the absence of Cdc20. Compared to the *cdc20mn* mutant, the *rad61-7A cdc20mn* mutant showed a delayed disappearance of the linear straining and an appearance of dotty Rec8 staining at late time points (Fig. 6, A and C). Again, linear Rec8 expression was frequently detected in Red1-negative nuclei of *rad61-7A cdc20mn* cells (Fig. 6A). The defective Rec8 release in *rad61-7A* mutants was also confirmed by Rec8-intensity measurements (Fig. 6B).

This *rad61-7A* defect resembles the *rec8-29A* mutant, although it is less pronounced than the *rad61* null mutant phenotype. The *rad61-7A rec8-29A* double mutant showed an even more delayed disappearance of Rec8 lines than the two single mutants (Fig. 6, A and C), indicating that both Rec8 and Rad61 phosphorylation contribute to Rec8 release in late prophase-I. The *rad61-7A* and the *rec8-29A* single mutant show 94% and 72.7% spore viability, respectively, while spore viability in the *rad61-7A rec8-29A* double mutant was reduced to 64.1% (Fig. S3, C and D). This confirms that the phosphorylation-triggered release is physiologically relevant for meiotic progression.

PLK promotes chromosome compaction in late prophase-I

To observe the consequences of Rec8-cohesin release in late prophase-I, we measured chromosome compaction using two fluorescently marked chromosome loci on chromosome IV in three strains, *ndt80*, *cdc20mn*, and

cdc5mn cdc20mn (Fig. 5D). At 0 h, the distance between the two loci was 1.55±0.42 μm in the *cdc20mn* mutant, and this was reduced to 1.28±0.41 μm at 5 h (Fig.5E) with no further decrease at 8 h in the *ndt80* mutant (1.26±0.45 [5 h] and 1.22±0.39 μm [8 h]). This is consistent with a compaction even that occurs in pachytene chromosomes (Challa et al., 2016). The *cdc20mn* showed an additional decrease of the distance to 0.58±0.27 μm at 8 h, or compaction to 37% of initial length. This argue for a specific chromosome compaction event of ~3-fold in prophase-I after pachytene. Importantly, this drastic chromosome compaction completely depends on Cdc5 PLK. The *cdc5mn cdc20mn* cells showed only mild compaction of chromosomes both at 5 and 8 h (Fig. 5, D and E).

Discussion

Our results suggest the existence of a phosphorylation-controlled step during late prophase-I/pro metaphase-I that leads to the partial release of cohesin in meiotic yeast cells. This occurs in addition to the previously identified two steps of cohesin release at metaphase/anaphase I and II (Fig. 7) (Buonomo et al., 2000; Klein et al., 1999). Prior to the final cleavage-dependent removal of cohesin, we show a cleavage-independent removal, which releases the meiotic kleisin subunit, Rec8, intact, at late prophase-I. This is meiotic “prophase-like pathway” as it is analogous to the “prophase” pathway in mitotic G2-phase and pro-metaphase of vertebrate cells (Haarhuis et al., 2014). Interestingly, mitotic cells in budding yeast seem to lack the prophase pathway (Lopez-Serra et al., 2013). This is consistent with the fact that budding yeast does not possess a sororin ortholog, the key regulator of cleavage-independent removal of cohesin during the late G2 phase in vertebrates (Nishiyama et al., 2010). While as vertebrate cells inactivate the Wapl inhibitor, sororin, in mitotic prophase, meiotic yeast cells appear to regulate the activity of Wapl, Rad61/Wpl1, positively by meiosis-specific phosphorylation, and also to control Rec8’s affinity to Smc3 negatively by meiosis-specific phosphorylation of Rec8.

Meiotic prophase-like pathway shares similar mechanism with the vertebrate prophase pathway

Similar to the vertebrate prophase pathway (Haarhuis et al., 2014), the meiotic prophase pathway for cohesin release in budding yeast is independent of cohesin cleavage. Rec8 was released from meiotic chromosomes in the absence of separase activity in Cdc20-depleted cells, as well as in cleavage-resistant *Rec8-N* cells. Moreover, we were able to recover the full-length Rec8 protein, which was stably bound to the chromatin during mid-pachytene, in chromatin-soluble factions during late prophase-I (Fig. 2A). These results show that a mechanism that releases Rec8-cohesin independent of kleisin cleavage exists.

Like the mammalian prophase pathway, the meiotic prophase pathway in yeast requires WAPL (Rad61/Wpl1) and PLK (Cdc5). During the mitotic G1 phase in yeast, Rad61/Wpl1 is known to promote the dissociation of mitotic cohesin (Lopez-Serra et al., 2013). During the mammalian mitotic prophase and the yeast G1 phase, the Wapl works together with Pds5 to mediate the opening of the exit gate between Scc1-Smc3 (Chan et al., 2012). Judged by the role of Rad61/Wpl1, we propose that the meiotic prophase pathway is mechanistically similar to the mammalian prophase pathway and the G1 pathway in yeast. The release of meiotic cohesin in late prophase-I may occur through the opening at the interface between Rec8 and Smc3 (Fig. 7). It might be possible to confirm this by expressing a Smc3-Rec8 fusion protein that locks the interface between the meiotic kleisin, Rec8, and Smc3.

Yeast meiotic prophase pathway is different from the mammalian prophase pathway

In vertebrate cells, sororin inactivation is essential for the cleavage-independent release of cohesin. Sororin is likely bound to the Scc1/Rad21 domain, to which Wapl also binds. Sororin binding sterically hinders the binding of Scc1/Rad21 to Wapl, and as a result, Wapl is unable to open the exit gate (Marston, 2014). Phosphorylated sororin dissociates from cohesin, allowing for binding between Wapl and Scc1, which leads to opening of the gate. Given that, budding yeast lacks sororin, the anti-cohesin activity of Rad61/Wpl1 in yeast is counteracted by Eco1-mediated acetylation of Smc3, which is sufficient to antagonize Rad61 activity in G2 phase (Rowland et al., 2009; Sutani et al., 2009). We found that

Smc3 acetylation is maintained during prophase-I (G2 phase) of meiosis (Fig 2A). Thus, rather than inactivating a negative regulator for Wpl, yeast meiotic cells seem to display a novel mechanism for cohesin release through enhancement of Rad61/Wpl1 activity. This enhancement correlates with the phosphorylation of the Rad61, which may either enhance Wapl activity directly and/or increase the interaction between Rec8 and Rad61.

We identified two critical regulators of the meiosis prophase pathway, Rad61 and PLK (Cdc5), which both are expressed during mitosis and meiosis. Nevertheless, our results show a meiosis-specific regulation of cohesin removal. Since, during meiosis, Scc1 is replaced by the meiosis-specific kleisin Rec8, we propose that Rec8 is an essential component for the meiosis-specific prophase pathway. In mitotic cells, PLK-dependent phosphorylation of Scc1 promotes its cleavage, rather than the release. Thus, the meiotic specificity of the prophase pathway is conferred by replacing Scc1 by Rec8.

In addition, Rad61 is phosphorylated only in meiotic prophase-I by the two mitotic kinases, DDK and PLK. Rec8 is known to interact directly with Cdc5/PLK (Katis et al., 2010). We also show that the meiosis-specific Cdc5-dependent phosphorylation of Rad61 requires Rec8. Therefore, Rec8 has dual functions in cohesin release during meiosis. Rec8 exhibits an intrinsic property that allows it to respond to the anti-cohesin activity of Wapl, as well as the ability to enhance Wapl activity by promoting its phosphorylation. The exact mechanism that induces the meiosis-specific, DDK-dependent phosphorylation of Rad61 in early prophase-I is unknown. We know that Rec8 at least does not play an essential role in this phosphorylation, as *rec8* mutants were able to initiate meiosis-specific DDK-dependent phosphorylation of Rad61. We propose that phosphorylation of Rad61 may augment anti-cohesin activities, and consequently, the gate-opening activity of the protein. In addition, we also propose that Rec8 phosphorylation may loosen the binding of Rec8 to Smc3 and Rad61 to unlock the Rec8-Smc3 gate.

The meiotic prophase pathway is conserved in higher eukaryotes

The cleavage-independent pathway of cohesin release during meiosis is conserved in higher eukaryotes such as nematodes, plants, and mammals. In

these organisms, differential distributions and/or reduced signals of cohesin on chromosomes or chromosome arms were observed in late prophase-I, as in diakinesis. In nematodes, cohesin on short arms, but not on long arms, is likely to be removed, in a manner dependent on aurora kinase, *air-2* (Rogers et al., 2002). Interestingly, in nematodes, Wapl (*wapl-1)*, controls the dynamics of kleisin COH3/4-containing cohesin, but not of cohesin associated with Rec8(Crawley et al., 2016). Immuno-staining showed that in *Arabidopsis thaliana*, most Rec8 molecules are released from meiotic chromosomes during the diplotene stage, and this is mediated by Wapl (De et al., 2014). Like yeast, *C. elegans* and *A. thaliana* lack a clear sororin ortholog, indicating that the removal of cohesin during meiosis is sororin-independent.

In mouse spermatocytes, the Rad21L kleisin, but not Rec8, is predominantly removed during the diplotene stage, in a manner partially dependent on PLK (Ishiguro et al., 2011). Recently, a novel regulatory circuit for cohesin removal was described during spermatogenesis, where Nek1 kinase-dependent “de”phosphorylation of Wapl promotes its retention on chromosomes and consequently the release of cohesin (Brieno-Enriquez et al., 2016). It was observed that during meiosis in mouse spermatocytes, phosphorylation of Wapl inhibits its activity. This is in sharp contrast to the role of Rad61 phosphorylation in the budding yeast, but may again reflect the absence of sororin in yeast.

Local regulation of protection and promotion of cohesin removal along the chromosomes

Results presented in this work showed that approximately 50-60% of chromosome-bound Rec8 at the pachytene stage can be dissociated from chromosomes during late prophase-I. On the other hand, 40-50% of Rec8 remains stably bound to chromosomes during late prophase-I, suggesting that these Rec8 molecules are either protected against or are not activated for the meiotic prophase-like pathway. Most of the chromatin-bound Rec8 at late prophase-I is still sensitive to artificially expressed separase while, as expected, Rec8 at kinetochores is resistant to it. At the onset of anaphase-I, kinetochore-bound Rec8 is protected by a molecule called Shugoshin (Sgo1)

(Katis et al., 2010; Kitajima et al., 2006), which is bound to kinetochores during late prophase-I. Indeed, artificial expression of separase in pachytene-arrested cells; e.g. *ndt80* mutant, completely removes Rec8 even at kinetochores (Yoon et al., 2016). Thus, the full protection of kinetochore-bound Rec8 is established only after the exit from mid-pachytene. In the mammalian prophase pathway, kinetochore-bound cohesin is protected by Shugoshin/PP2A which dephosphorylates subunits like sororin. A similar protection mechanism seen in the mammalian mitotic prophase pathway may also operate on cohesins that are bound to meiotic chromosome arms and to the kinetochores. However, protection of arm cohesin, which is sensitive to separase, must be functionally distinct from kinetochore-cohesin, which is not.

The meiotic prophase pathway requires DDK- and PLK-dependent meiosis-specific phosphorylation of Rec8 and Rad61. Indeed, we showed that the Rec8 released from chromosomes is more phosphorylated than the complement that remains tightly bound to chromosomes. One plausible mechanism for the observed protection against the prophase pathway is local activation of dephosphorylation of cohesin, as seen at kinetochores, where Shugoshin recruits the phosphatase PP2A. This is similar to the role that Sgo1 plays in protection of centromeric cohesin at the onset of anaphase-I in vertebrate meiosis.

Alternatively, local activation by phosphorylation of Rec8 and Rad61 may be a mechanism that promotes cohesin release in distinct chromosomal regions. For instance, local removal of cohesion at the site of chiasmata (Kleckner, 2006) may be a necessary step in the formation of normal diplotene bivalents.

Is Rec8 phosphorylation indeed required for the cleavage by separase?

Previous reports strongly suggested that phosphorylation of Rec8 by DDK, PLK, and CK1 is essential for cleavage by separase (Brar et al., 2006; Katis et al., 2010). However, this was not directly tested by an *in vitro* cleavage assay. Our results presented here suggest that Rec8 phosphorylation by DDK and PLK is for Rec8-cohesin dissociation at late prophase-I. However, we and others (Yoon et al., 2016) also shows that chromosome-bound Rec8 with reduced phosphorylation can be used as a substrate for separase-mediated cleavage *in*

vivo, since ectopic expression of separase in late prophase-I was sufficient for the removal of Rec8-cohesin from chromosome arms, but not from centromeres (Fig. 2D). Thus, it is possible that phosphorylation of Rec8 plays a major role in cleavage-independent dissociation of cohesin, rather than triggering it for cleavage by separase.

Functions of the meiotic prophase pathway

Given that cohesin at the chromosome arm is important for chromosome segregation in MI, one may suggest that the meiotic-prophase pathway is dangerous in meiotic cells, and thus, it is important to ask why meiosis has retained this dangerous pathway. It is known that during late prophase-I, which corresponds to diplotene and diakinesis in other organisms, drastic changes in chromosome morphology occur (Zickler and Kleckner, 1999). This includes strong compaction while chiasmata emerge, to prepare for chromosome segregation. In meiosis I, the chiasmata are essential for chromosome segregation. Indeed, loss of cohesion around chiasmata sites has been observed in various organisms (Kleckner, 2006). Similarly, in worms, Wapl-dependent cohesin removal promotes recombination-mediated change of meiotic chromosome structure (Crawley et al., 2016).

We propose that one function of cohesin release in late prophase-I is to promote chiasma formation. Since the individualization of chromosomes may be important for of chiasmata. In addition, in late prophase-I, chromosomes show drastic compaction. Even in the budding yeast, late meiotic chromosomes are compacted by approximately 3 fold as compared with their sizes in meiotic G1 (this study) (Yu and Koshland, 2005). Concomitant with this drastic compaction, condensin has been shown to bind to meiotic chromosomes following the pachytene stage (Jin et al., 2009; Yu and Koshland, 2005). The binding of condensin not only promotes condensation, but also facilitates the release of cohesin (Yu and Koshland, 2005), and may promote individualization of chromatids. In this work we show that Cdc5 depletion causes both a failure in the meiotic prophase pathway and a defect in chromosome compaction. This is consistent with a role of cohesin removal in compaction, although other interpretations are possible. What the basic propose of cohesin removal is in

prophase, either to make space for condensin, to allow chiasma morphogenesis, to allow compaction or another function, remains to be answered in future studies.

Materials and Methods

Strains and strain construction

All strains described here are derivatives of SK1 diploid strains, MSY832/833 (*MATα/MAT**a**, ho::LYS2/", lys2/", ura3/", leu2::hisG/", trp1::hisG/"*). Strain genotypes are given in Table S1. *CEN4-GFP/TEL4-GFP* and Esp1-overexpression strains was provided by Dr. Doug Koshland and Dr. Keun P. Kim, respectively.

Antisera and antibodies

Anti-Zip1, anti-Red1, and anti-Rec8 antisera for cytology and western blotting have been described previously(Shinohara et al., 2008; Zhu et al., 2011). Secondary antibodies conjugated with Alxea488 and Alexa594 dyes (Molecular Probes, Life Technologies, UK) were used for the detection of the primary antibodies. Anti-Rec8-pS179 (PLK site) and anti-Rec8-pS521 (DDK site) were generous gifts from Dr. Angelika Amon (MIT). Anti-acetyl-Smc3 was a gift by Dr. Katsu Shirahige (U. of Tokyo). Anti-Rad61-PS69-pS70 antibody was raised in rabbit using a Rad61 peptide containing pS69 and pS70 by a company (MBL Co. Ltd).

Cytology

Immunostaining of chromosome spreads was performed as described previously(Shinohara et al., 2000; Shinohara et al., 2003). Stained samples were observed using an epi-fluorescence microscope (BX51; Olympus, Japan) with a 100X objective (NA1.3). Images were captured by CCD camera (CoolSNAP; Roper, USA), and afterwards processed using IP lab and/or iVision (Sillicon, USA), and Photoshop (Adobe, USA) software tools.

SIM imaging

The structured illumination microscopy was carried out using super resolution-structured illumination (SR-SIM) microscope (Elyra S.1 [Zeiss], Plan-Apochromat 63x/1.4 NA objective lens, EM-CCD camera [iXon 885; Andor Technology], and ZEN Blue 2010D software [Zeiss]) at Friedrich Miescher

Institute for Biomedical Research, Switzerland. Image Processing was performed with Zen software (Zeiss, Germany], image J and Photoshop.

Fluorescence intensity measurement

Mean fluorescence of the whole nucleus was quantified with Image J. Quantification was performed using unprocessed raw images and identical exposure time setting in DeltaVision system (Applied Precision, USA). The area of a nuclear spread was defined as an oval, and the mean fluorescence intensity was measured within this area.

Chromatin fractionation

Chromatin fractionation was performed as described previously(Kee et al., 2004). The cells were digested with Zymolyase 100T (Nakarai Co. Ltd) and the spheroplasts were pelleted. The pellets were resuspended in five volumes of hypotonic buffer (HB; 100 mM MES-NaOH, pH 6.4, 1 mM EDTA, 0.5 mM $MgCl_2$) supplemented with a protease inhibitor cocktail (Sigma, USA). After 5 min, 120 µl of whole cell extract (WCE) were layered onto 120 µl of 20% (W/V) sucrose in HB and centrifuged for 10 min at 16,000 *g*. The supernatants were saved and the pellets were resuspended in 120 µl EBX buffer (50 mM HEPS-NaOH, pH 7.4, 100 mM KCl, 1 mM EDTA, 2.5 mM $MgCl_2$, 0.05% Triton X100) and centrifuged for 10 min at 16,000 *g*. The pellets were again collected and resuspended in EBX buffer with 5 units/ml DNase I and 1 mM $MgCl_2$ for 5 min. The supernatants were saved for further analysis.

Compaction assay

For distance measurements on probed SCs at 0, 5 and 8 h, chromosome spreads were prepared as described above and stained with both anti-Rec8 and anti-GFP antibodies. The distance between two GFP foci on chromosome IV was measured by Velocity^{TM} programm (Applied Precision, USA) or IPLab (Sillicon, USA).

Yeast culture

Yeast cell culture and time-course analyses of the events during meiosis and the

cell cycle progression were performed as described previously(Shinohara et al., 2003).

Statistics

Means ± S.D values are shown. Datasets were compared using the Mann-Whitney U-test. χ^2-test was used for proportion. Multiple test correction was done with Bonferroni's correction. *, **, and *** show P-values of <0.05, <0.01 and <0.001, respectively. The results of all statistical tests are shown in Supplemental Table 2.

Supplemental Information

Supplemental information includes Supplemental three figures and two tables can be found with the article online at.

References

Arguello-Miranda, O., I. Zagoriy, V. Mengoli, J. Rojas, K. Jonak, T. Oz, P. Graf, and W. Zachariae. 2017. Casein Kinase 1 Coordinates Cohesin Cleavage, Gametogenesis, and Exit from M Phase in Meiosis II. *Dev Cell*. 40:37-52.

Attner, M.A., M.P. Miller, L.S. Ee, S.K. Elkin, and A. Amon. 2013. Polo kinase Cdc5 is a central regulator of meiosis I. *Proc Natl Acad Sci U S A*. 110:14278-14283.

Brar, G.A., A. Hochwagen, L.S. Ee, and A. Amon. 2009. The multiple roles of cohesin in meiotic chromosome morphogenesis and pairing. *Mol Biol Cell*. 20:1030-1047.

Brar, G.A., B.M. Kiburz, Y. Zhang, J.E. Kim, F. White, and A. Amon. 2006. Rec8 phosphorylation and recombination promote the step-wise loss of cohesins in meiosis. *Nature*. 441:532-536.

Brieno-Enriquez, M.A., S.L. Moak, M. Toledo, J.J. Filter, S. Gray, J.L. Barbero, P.E. Cohen, and J.K. Holloway. 2016. Cohesin Removal along the Chromosome Arms during the First Meiotic Division Depends on a NEK1-PP1gamma-WAPL Axis in the Mouse. *Cell Rep*. 17:977-986.

Buonomo, S.B., R.K. Clyne, J. Fuchs, J. Loidl, F. Uhlmann, and K. Nasmyth. 2000. Disjunction of homologous chromosomes in meiosis I depends on proteolytic cleavage of the meiotic cohesin Rec8 by separin. *Cell*. 103:387-398.

Challa, K., M.S. Lee, M. Shinohara, K.P. Kim, and A. Shinohara. 2016. Rad61/Wpl1 (Wapl), a cohesin regulator, controls chromosome compaction during meiosis. *Nucleic Acids Res*. 44:3190-3203.

Chan, K.L., M.B. Roig, B. Hu, F. Beckouet, J. Metson, and K. Nasmyth. 2012. Cohesin's DNA exit gate is distinct from its entrance gate and is regulated by acetylation. *Cell*. 150:961-974.

Clyne, R.K., V.L. Katis, L. Jessop, K.R. Benjamin, I. Herskowitz, M. Lichten, and K. Nasmyth. 2003. Polo-like kinase Cdc5 promotes chiasmata formation and cosegregation of sister centromeres at meiosis I. *Nat Cell Biol*. 5:480-485.

Crawley, O., C. Barroso, S. Testori, N. Ferrandiz, N. Silva, M. Castellano-Pozo,

A.L. Jaso-Tamame, and E. Martinez-Perez. 2016. Cohesin-interacting protein WAPL-1 regulates meiotic chromosome structure and cohesion by antagonizing specific cohesin complexes. *Elife*. 5:e10851.

De, K., L. Sterle, L. Krueger, X. Yang, and C.A. Makaroff. 2014. Arabidopsis thaliana WAPL is essential for the prophase removal of cohesin during meiosis. *PLoS Genet*. 10:e1004497.

Gandhi, R., P.J. Gillespie, and T. Hirano. 2006. Human Wapl is a cohesin-binding protein that promotes sister-chromatid resolution in mitotic prophase. *Curr Biol*. 16:2406-2417.

Gladstone, M.N., D. Obeso, H. Chuong, and D.S. Dawson. 2009. The synaptonemal complex protein Zip1 promotes bi-orientation of centromeres at meiosis I. *PLoS Genet*. 5:e1000771.

Gruber, S., P. Arumugam, Y. Katou, D. Kuglitsch, W. Helmhart, K. Shirahige, and K. Nasmyth. 2006. Evidence that loading of cohesin onto chromosomes involves opening of its SMC hinge. *Cell*. 127:523-537.

Gruber, S., C.H. Haering, and K. Nasmyth. 2003. Chromosomal cohesin forms a ring. *Cell*. 112:765-777.

Haarhuis, J.H., A.M. Elbatsh, and B.D. Rowland. 2014. Cohesin and its regulation: on the logic of X-shaped chromosomes. *Dev Cell*. 31:7-18.

Ishiguro, K., J. Kim, S. Fujiyama-Nakamura, S. Kato, and Y. Watanabe. 2011. A new meiosis-specific cohesin complex implicated in the cohesin code for homologous pairing. *EMBO Rep*. 12:267-275.

Jin, H., V. Guacci, and H.G. Yu. 2009. Pds5 is required for homologue pairing and inhibits synapsis of sister chromatids during yeast meiosis. *J Cell Biol*. 186:713-725.

Katis, V.L., J.J. Lipp, R. Imre, A. Bogdanova, E. Okaz, B. Habermann, K. Mechtler, K. Nasmyth, and W. Zachariae. 2010. Rec8 phosphorylation by casein kinase 1 and Cdc7-Dbf4 kinase regulates cohesin cleavage by separase during meiosis. *Dev Cell*. 18:397-409.

Kee, K., R.U. Protacio, C. Arora, and S. Keeney. 2004. Spatial organization and dynamics of the association of Rec102 and Rec104 with meiotic chromosomes. *The EMBO journal*. 23:1815-1824.

Kitajima, T.S., S.A. Kawashima, and Y. Watanabe. 2004. The conserved

kinetochore protein shugoshin protects centromeric cohesion during meiosis. *Nature*. 427:510-517.

Kitajima, T.S., T. Sakuno, K. Ishiguro, S. Iemura, T. Natsume, S.A. Kawashima, and Y. Watanabe. 2006. Shugoshin collaborates with protein phosphatase 2A to protect cohesin. *Nature*. 441:46-52.

Kleckner, N. 2006. Chiasma formation: chromatin/axis interplay and the role(s) of the synaptonemal complex. *Chromosoma*. 115:175-194.

Klein, F., P. Mahr, M. Galova, S.B. Buonomo, C. Michaelis, K. Nairz, and K. Nasmyth. 1999. A central role for cohesins in sister chromatid cohesion, formation of axial elements, and recombination during yeast meiosis. *Cell*. 98:91-103.

Kueng, S., B. Hegemann, B.H. Peters, J.J. Lipp, A. Schleiffer, K. Mechtler, and J.M. Peters. 2006. Wapl controls the dynamic association of cohesin with chromatin. *Cell*. 127:955-967.

Lee, B.H., and A. Amon. 2003. Role of Polo-like kinase CDC5 in programming meiosis I chromosome segregation. *Science*. 300:482-486.

Lee, J., and T. Hirano. 2011. RAD21L, a novel cohesin subunit implicated in linking homologous chromosomes in mammalian meiosis. *J Cell Biol*. 192:263-276.

Loidl, J. 2016. Conservation and Variability of Meiosis Across the Eukaryotes. *Annu Rev Genet*. 50:293-316.

Lopez-Serra, L., A. Lengronne, V. Borges, G. Kelly, and F. Uhlmann. 2013. Budding yeast Wapl controls sister chromatid cohesion maintenance and chromosome condensation. *Curr Biol*. 23:64-69.

Marston, A.L. 2014. Chromosome segregation in budding yeast: sister chromatid cohesion and related mechanisms. *Genetics*. 196:31-63.

Marston, A.L. 2015. Shugoshins: tension-sensitive pericentromeric adaptors safeguarding chromosome segregation. *Mol Cell Biol*. 35:634-648.

Montagnoli, A., B. Valsasina, D. Brotherton, S. Troiani, S. Rainoldi, P. Tenca, A. Molinari, and C. Santocanale. 2006. Identification of Mcm2 phosphorylation sites by S-phase-regulating kinases. *J Biol Chem*. 281:10281-10290.

Nishiyama, T., R. Ladurner, J. Schmitz, E. Kreidl, A. Schleiffer, V. Bhaskara, M.

Bando, K. Shirahige, A.A. Hyman, K. Mechtler, and J.M. Peters. 2010. Sororin mediates sister chromatid cohesion by antagonizing Wapl. *Cell*. 143:737-749.

Nishiyama, T., M.M. Sykora, P.J. Huis in 't Veld, K. Mechtler, and J.M. Peters. 2013. Aurora B and Cdk1 mediate Wapl activation and release of acetylated cohesin from chromosomes by phosphorylating Sororin. *Proc Natl Acad Sci U S A*. 110:13404-13409.

Riedel, C.G., V.L. Katis, Y. Katou, S. Mori, T. Itoh, W. Helmhart, M. Galova, M. Petronczki, J. Gregan, B. Cetin, I. Mudrak, E. Ogris, K. Mechtler, L. Pelletier, F. Buchholz, K. Shirahige, and K. Nasmyth. 2006. Protein phosphatase 2A protects centromeric sister chromatid cohesion during meiosis I. *Nature*. 441:53-61.

Rockmill, B., and G.S. Roeder. 1988. RED1: a yeast gene required for the segregation of chromosomes during the reductional division of meiosis. *Proc Natl Acad Sci U S A*. 85:6057-6061.

Rogers, E., J.D. Bishop, J.A. Waddle, J.M. Schumacher, and R. Lin. 2002. The aurora kinase AIR-2 functions in the release of chromosome cohesion in Caenorhabditis elegans meiosis. *J Cell Biol*. 157:219-229.

Rowland, B.D., M.B. Roig, T. Nishino, A. Kurze, P. Uluocak, A. Mishra, F. Beckouet, P. Underwood, J. Metson, R. Imre, K. Mechtler, V.L. Katis, and K. Nasmyth. 2009. Building sister chromatid cohesion: smc3 acetylation counteracts an antiestablishment activity. *Mol Cell*. 33:763-774.

Shinohara, M., S.L. Gasior, D.K. Bishop, and A. Shinohara. 2000. Tid1/Rdh54 promotes colocalization of rad51 and dmc1 during meiotic recombination. *Proc Natl Acad Sci U S A*. 97:10814-10819.

Shinohara, M., S.D. Oh, N. Hunter, and A. Shinohara. 2008. Crossover assurance and crossover interference are distinctly regulated by the ZMM proteins during yeast meiosis. *Nat Genet*. 40:299-309.

Shinohara, M., K. Sakai, T. Ogawa, and A. Shinohara. 2003. The mitotic DNA damage checkpoint proteins Rad17 and Rad24 are required for repair of double-strand breaks during meiosis in yeast. *Genetics*. 164:855-865.

Sutani, T., T. Kawaguchi, R. Kanno, T. Itoh, and K. Shirahige. 2009. Budding yeast Wpl1(Rad61)-Pds5 complex counteracts sister chromatid

cohesion-establishing reaction. *Curr Biol*. 19:492-497.

Sym, M., J.A. Engebrecht, and G.S. Roeder. 1993. ZIP1 is a synaptonemal complex protein required for meiotic chromosome synapsis. *Cell*. 72:365-378.

Tachibana-Konwalski, K., J. Godwin, L. van der Weyden, L. Champion, N.R. Kudo, D.J. Adams, and K. Nasmyth. 2010. Rec8-containing cohesin maintains bivalents without turnover during the growing phase of mouse oocytes. *Genes Dev*. 24:2505-2516.

Trelles-Sticken, E., C. Adelfalk, J. Loidl, and H. Scherthan. 2005. Meiotic telomere clustering requires actin for its formation and cohesin for its resolution. *J Cell Biol*. 170:213-223.

Xu, L., M. Ajimura, R. Padmore, C. Klein, and N. Kleckner. 1995. NDT80, a meiosis-specific gene required for exit from pachytene in Saccharomyces cerevisiae. *Mol Cell Biol*. 15:6572-6581.

Yoon, S.W., M.S. Lee, M. Xaver, L. Zhang, S.G. Hong, Y.J. Kong, H.R. Cho, N. Kleckner, and K.P. Kim. 2016. Meiotic prophase roles of Rec8 in crossover recombination and chromosome structure. *Nucleic Acids Res*. 44:9296-9314.

Yu, H.G., and D. Koshland. 2005. Chromosome morphogenesis: condensin-dependent cohesin removal during meiosis. *Cell*. 123:397-407.

Zhu, Z., S. Mori, H. Oshiumi, K. Matsuzaki, M. Shinohara, and A. Shinohara. 2011. Cyclin-dependent kinase promotes formation of the synaptonemal complex in yeast meiosis. *Genes Cells*. 15:1036-1050.

Zickler, D., and N. Kleckner. 1999. Meiotic chromosomes: integrating structure and function. *Annu Rev Genet*. 33:603-754.

AUTHOR CONTRIBUTIONS

K.C., M.S., and A.S. designed the experiments. K.C., G.F.V., and A.S. performed the experiments and analysed the data. M.S. and F.K. provided materials. K.C., with help by S.G. carried out SIM analysis. K.C., M.S., F.K., S.G., and A.S. prepared the manuscript.

ACKNOWLEDGEMENTS

We are grateful to Drs. A. Marston, K. Matsuzaki, and H. B. D. P. Rao as well as the members of the Shinohara lab for helpful discussions. We thank Drs. A. Seeber and L. Gelman for help with SIM and Ms. A. Murakami and H. Wakabayashi for excellent technical assistance. We are grateful to Drs. A. Amon, K. Kim, D. Koshland, K. Shirahige, K. Nasmyth, and W. Zachariae for materials used in this study. K.C. and G.F.V. were supported by Institute for Protein Research, Osaka University. This work was supported by JSPS KAKENHI Grant Number; 22125001, 22125002, 15H05973 and 16H04742 to A.S. M.S. was supported by the Japan Society for the Promotion of Science (JSPS) through the Funding Program for Next Generation World-Leading Researchers (NEXT Program).

Conflict of interest

The authors declare that they have no conflict of interest.

Figure Legends

Figure 1. Rec8 shows dynamic localization in late meiotic prophase-I

A. Immunostaining analysis of Rec8 (red) and axis protein Red1 (green; top) and Rec8 (red) and SC protein Zip1 (green; bottom) in *cdc20-mn* (KSY642/643) strain. Representative image with or without DAPI (blue) dye is shown. Rec8 staining in the *cdc20-mn* was classified as linear (5 h) and altered (8 h) classes. The bar indicates 2 μm.

B. Kinetics of Rec8 (left), Zip1 (middle) and Red1 (right) staining in *cdc20-mn* (KSY642/643) strain was analyzed. A minimum 100 cells were counted at each time point. Error bars (Rec8) show the standard deviation (S.D.; n=3). Zip1 staining is classified as follows: dotty (blue); short linear (green); full linear staining (red). Red1 staining is classified as follows; dotty (light blue); short linear (light purple); full linear staining (purple).

C. Total signal intensity of Rec8, and DAPI in image shown in (A) was measured in *cdc20-mn* (KSY642/643) cells. A minimum 30 nuclei were quantified in representative time points. Error bars show the S.D. (n=3).

D. SR-SIM microscopic observation of Rec8 (red) and Ctf19 (green) (left) in *cdc20-mn* (KSY642/643) and *ndt80* (KSY467/468) cells. Representative image with or without DAPI (blue) dye is shown. White insets are shown in a magnified view at right. The bar indicates 2μm.

E. Total signal intensity of Rec8 and DAPI in image shown (D) was measured in *cdc20-mn* (KSY642/643) and *ndt80* (KSY467/468) cells as shown in (C).

F. Immunostaining analysis of Rec8 (red) and Red1 (green) in wild type (MSY832/833) cells. Representative image with or without DAPI (blue) dye is shown. Rec8 staining was classified as linear (5 h) and altered (6 h) classes with Red1-positive and -negative, respectively. The bar indicates 2 μm.

G. Kinetics of Rec8 and Red1 positive spreads in wild type (MSY832/833) is shown. A minimum 100 nuclei were quantified in representative time points. Error bars show the S.D. (n=3).

H. Quantification of total Rec8 and DAPI signal intensity in Red1-postive and Red1-negative spreads in wild type was analyzed as shown in (C).

I. Localization of Rec8 (red) in *REC8-N* (KSY597) mutants.

J. Quantification of total Rec8 and DAPI signal intensity in *REC8-N* (KSY597) was analyzed as shown in (C).

Figure 2. Rec8 dissociates from meiotic chromosomes at late prophase-I

A. Chromatin fractionation assay was carried out using *cdc20-mn* (KSY642/643) and *ndt80* (KSY467/468) mutant cells. Western blotting was performed for whole cell extracts (W), soluble fractions (S) and chromatin-bound fraction (P). Rec8 (top) and acetyl-Smc3 (second) were probed together with tubulin (third) and Histone 2B (H2B; bottom) as controls for soluble and chromatin-bound proteins, respectively. Two major phosphorylated Rec8 bands are indicated with red and green bars on the left.

B. Quantification of Rec8 band intensity in (A) is shown. Rec8-enrichment to chromatin is expressed as a ratio of Rec8 to H2B levels while the soluble fraction of Rec8 is based on the ratio of Rec8 to tubulin levels. Rec8 level in *cdc20-mn* strain whole cell extracts (W) at 5 h was used to normalize the values. Error bars show the S.D. (n=3).

C. Intensity of acetyl-Smc3 shown in (A) was quantified and analyzed as described in (B).

D. Single culture of *cdc20-mn pCUP-Esp1-9myc* (KSY1009/1010) strain was synchronized and divided into two cultures; then Esp1 expression was induced by addition of 50 μM $CuSO_4$ at 3 and 5 h. Prepared chromosome spreads were immuno-stained for Rec8 (red) and Ctf19 (green). Representative images are shown. The bar indicates 2 μm.

E. Total Rec8 and DAPI signal intensity was quantified as shown in Fig. 1C. A minimum 30 nuclei were quantified in each representative time points. Error bars show the S.D. (n=3).

F. Chromatin fractionation assay of *cdc20-mn pCUP-Esp1-9myc* (KSY1009/1010) cells without and with overexpression of Esp1 was carried out as shown in (A).

G. Quantification of Rec8 levels in *cdc20-mn pCUP-ESP1-9myc* (KSY1009/1010) strain (G) was analyzed as shown in (B). Whole cell extracts (W) at 5 h sample was used for normalization.

Figure 3. Rec8 phosphorylation is required for efficient dissociation of Rec8 at late prophase-I

A. Chromatin fractionation assay for *cdc20-mn* (KSY642/643) and *cdc20-mn cdc5-mn* (KSY659/660) mutant cells was carried out as described in Fig. 2A.

B. Quantification of Rec8 band intensity in (A) is performed as shown in Fig. 2B. Error bars show the S.D. (n=3).

C. Localization of Rec8 (red) and Rec8-pS521 (green) was analyzed in *cdc20-mn* (KSY642/643) *cdc20-mn cdc5-mn* (KSY659/660) cells.

D. Total Rec8, Rec8-pS521, and DAPI signal intensity in (C) was studied as in Fig. 1C. Error bars show the S.D.

E. Localization of Rec8 (red) in *CDC20-mn* (KSY642/643) and *CDC20-mn CDC5-mn* (KSY659/660) mutants. Representative image is shown. The bar indicates 2 μm.

F. Kinetics of Rec8 in (E) was classified as shown in Fig. 1B. Error bars show the S.D. (n=3).

G. Total Rec8 and DAPI signal intensity was quantified as shown in Fig. 1C. A minimum 30 nuclei were quantified in each representative time points. Error bars show the S.D. (n=3).

Figure 4. Rec8 phosphorylation is critical for cleavage-independent Rec8 dissociation from meiotic chromosomes

A. Localization of Rec8 (red) and Red1 (green) on chromosome spreads was analyzed for *CDC20-mn* (KSY642/643) and *CDC20-mn rec8-29A* (KSY866/867) cells. Representative image with or without DAPI (blue) dye is shown. The bar indicates 2μm.

B. Kinetics of Rec8 and Red1 staining classes in (A) was analyzed as in Fig. 1b. A minimum 100 cells were analyzed at each time point. Error bars show the S.D. (n=3).

C. Localization of Rec8 (red) and Zip1 (green) spreads was studied in *CDC20-mn* (KSY642/643) and *CDC20-mn rec8-29A* (KSY866/867).

D. Kinetics of Zip1 staining in (F) was classified shown as in Fig. 1b. Error bars show the variation from two independent experiments.

E. Localization of Rec8 (red) and Ctr19 (green) was examined in *CDC20-mn* (KSY642/643) and *CDC20-mn rec8-29A* (KSY866/867) cells.

F. Kinetics of Rec8 (left) in (E) was analyzed as in Fig. 1b.

G. Total Rec8 and DAPI signal intensity was quantified as described in Fig. 1C. Error bars show the S.D. (n=3).

Figure 5. Cdc5 is sufficient for cleavage-independent Rec8 dissociation from meiotic chromosomes

A. Localization of Rec8 (red) with or without DAPI (blue) in *ndt80* (KSY467/468), *ndt80 GALp-CDC5 GAL4-DB-ER* without estradiol induction (-ER) (KSY887/888), *ndt80 GALp-CDC5-N209A GAL4-DB-ER* with estradiol induction (+ER) (KSY882/883) and *ndt80 GALp-CDC5 GAL4-DB-ER* (-ER) (KSY887/888) cells is shown. *CDC5* overexpression was induced by the addition of 400 nM Estradiol at 2 h.

B. Kinetics of Rec8 classes in (A) was classified shown in Fig. 1b. A minimum 100 cells were counted at each time point.

C. Expression profiles of Cdc5 during meiosis were verified by western blotting in *ndt80* (KSY467/468), *ndt80 Galp-CDC5 GAL4-DB-ER* without estradiol induction (-ER) (KSY887/888), *ndt80 GALp-CDC5-N209A GAL4-DB-ER* with estradiol induction (+ER) (KSY882/883) and *ndt80 GALp-CDC5 GAL4-DB-ER* (-ER) (KSY887/888) cells is shown. *CDC5* overexpression was induced by the addition of 400nM Estradiol at 2 h. At each time point of meiosis, cells were fixed with trichloroacetic acid (TCA), and cell lysates were examined. Tubulin used was utilized as a loading control. The protein positions are indicated with the lines on the right.

D. Representative images of *CEN4* and *TEL4* GFP foci (green) and nuclei (blue) in *cdc20-mn* (KSY991/642), *ndt80* (KSY445/467) and *cdc20-mn CDC5-mn* (KSY989/659) cells in a single focal plane of whole cell staining at each time point are shown. The bar indicates 2μm.

E. Distances between *CEN4* and *TEL4* at each time point 0h, 5h, 8h (*cdc20-mn;* KSY991/642 and *ndt80;* KSY445/467) 10 h in *cdc20-mn CDC5-mn* (KSY989/659) were measured and plotted as a box/whisker plot. A minimum 100 nuclei were studied in each time point.

Figure 6. Rad61/Wpl1 plays a role in cohesin-release in late prophase-I.

A. Localization of Rec8 (red) and Ctf19 (green) in *cdc20-mn* (KSY642/643), *cdc20-mn rad61* (KSY637/638), *cdc20-mn rad61-7A* (KSY653/654) and *cdc20-mn rec8-29A rad61-7A* (KSY1043/1044) cells. Representative image for each strain at various time points are shown.

B. Measurement of total Rec8 and DAPI signal intensity in (a) was analyzed in Fig.1c. Error bars show the S.D. (n=3).

C. Kinetics of Rec8-classes was studied as described in Fig. 1b. A minimum 100 cells were analyzed per time point. Error bars show the S.D. (n=3).

D. Expression profiles of Rec8 and Rad61-Flag during meiosis were verified using *RAD61-FLAG* (KSY440/441) cells by western blotting. The protein positions are indicated with the lines on the right. Phosphorylated species of Rec8 and Rad61-Flag are shown by arrows.

E. Bands shits of Rec8 and Rad61 in *RAD61-FLAG* (KSY440/441) and *cdc5-mn RAD61-FLAG* (KSY434/435) cells were studied as shown in (D).

F. Bands shits of Rec8 and Rad61 were analyzed in presence and absence of 1NM-PP1 in *RAD61-FLAG* (KSY440/441) and *cdc7-as3 RAD61-FLAG* (KSY978/979) strains at the indicated time points by western blotting as shown in (D).

G. The western blotting analysis was carried out for Rad61-Flag (Right) and Rad61-pS69, 70 (left) in *RAD61-FLAG* (KSY440/441), *rad61-S69A, S70A-FLAG* (KSY754/757) and *rad61-7A-FLAG* (KSY753/755) strains as shown in (D).

H. Bands shits of Rec8 and Rad61 in *RAD61-FLAG* (KSY440/441) and *rec8 RAD61-FLAG* (KSY627/628) cells were analyzed as shown in (A).

Figure 7. A model for meiotic prophase-like pathway at late prophase-I

See more detail in text.

Challa et al. Figure 1

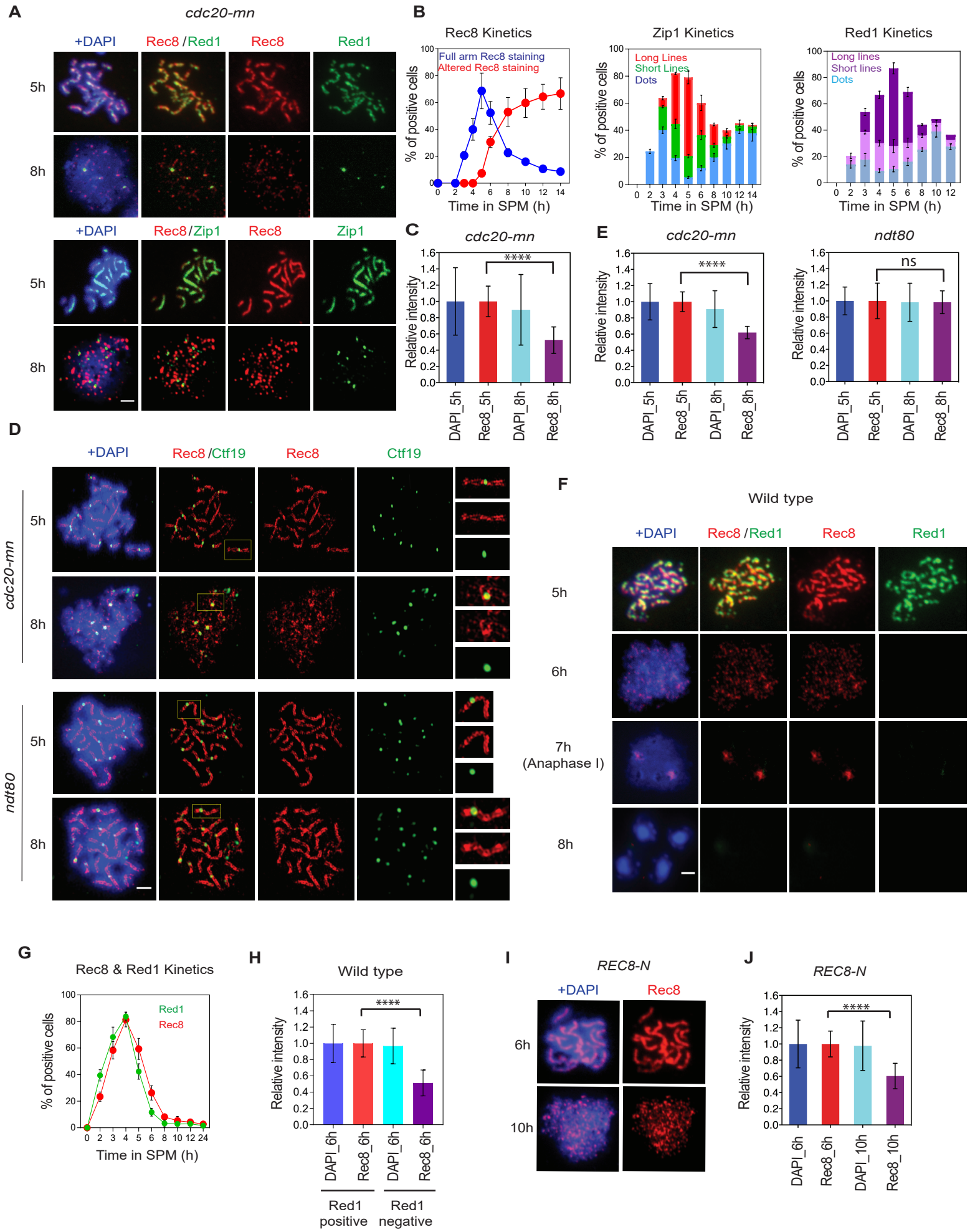

Challa et al. Figure 2

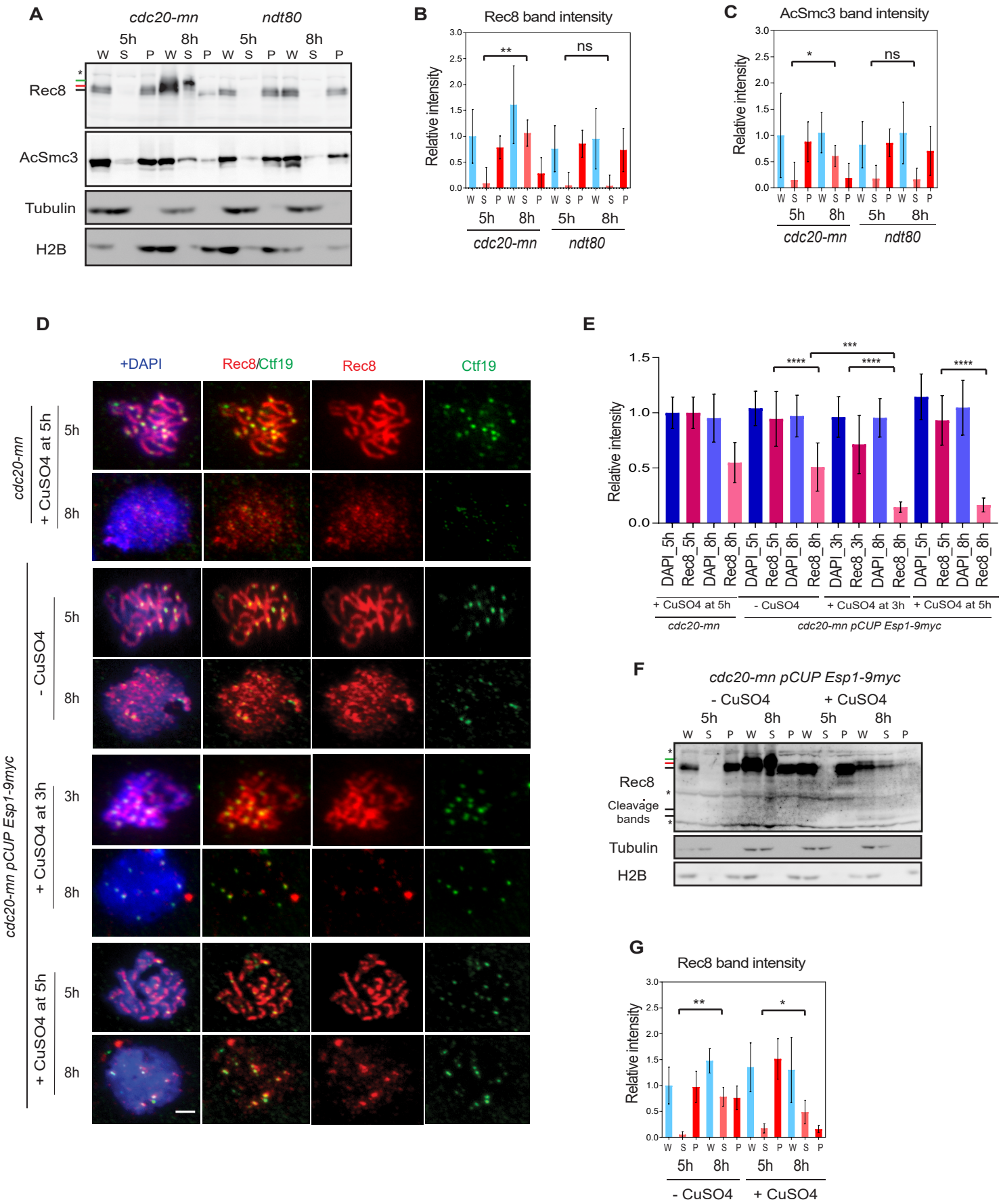

Challa et al. Figure 3

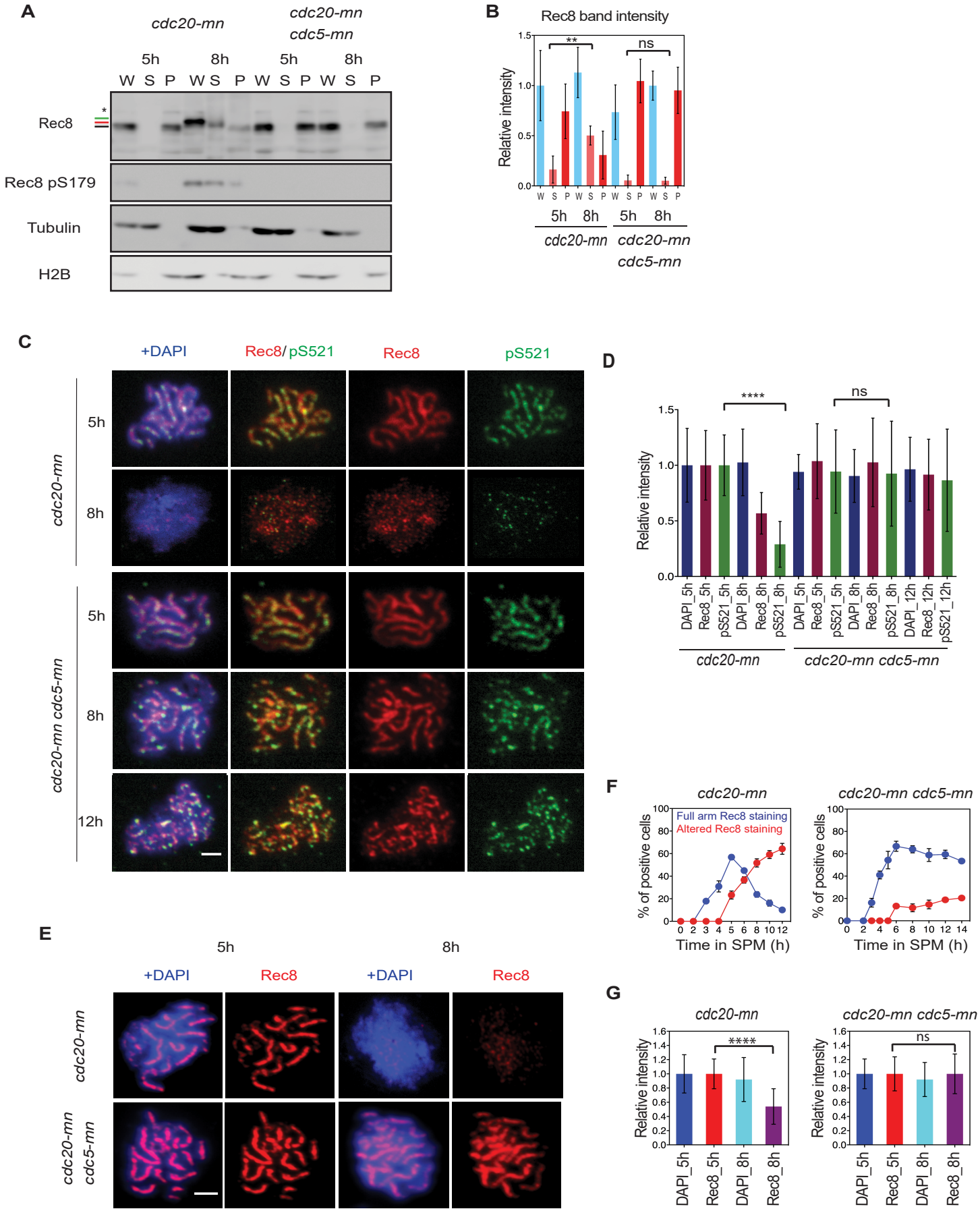

Challa et al. Figure 4

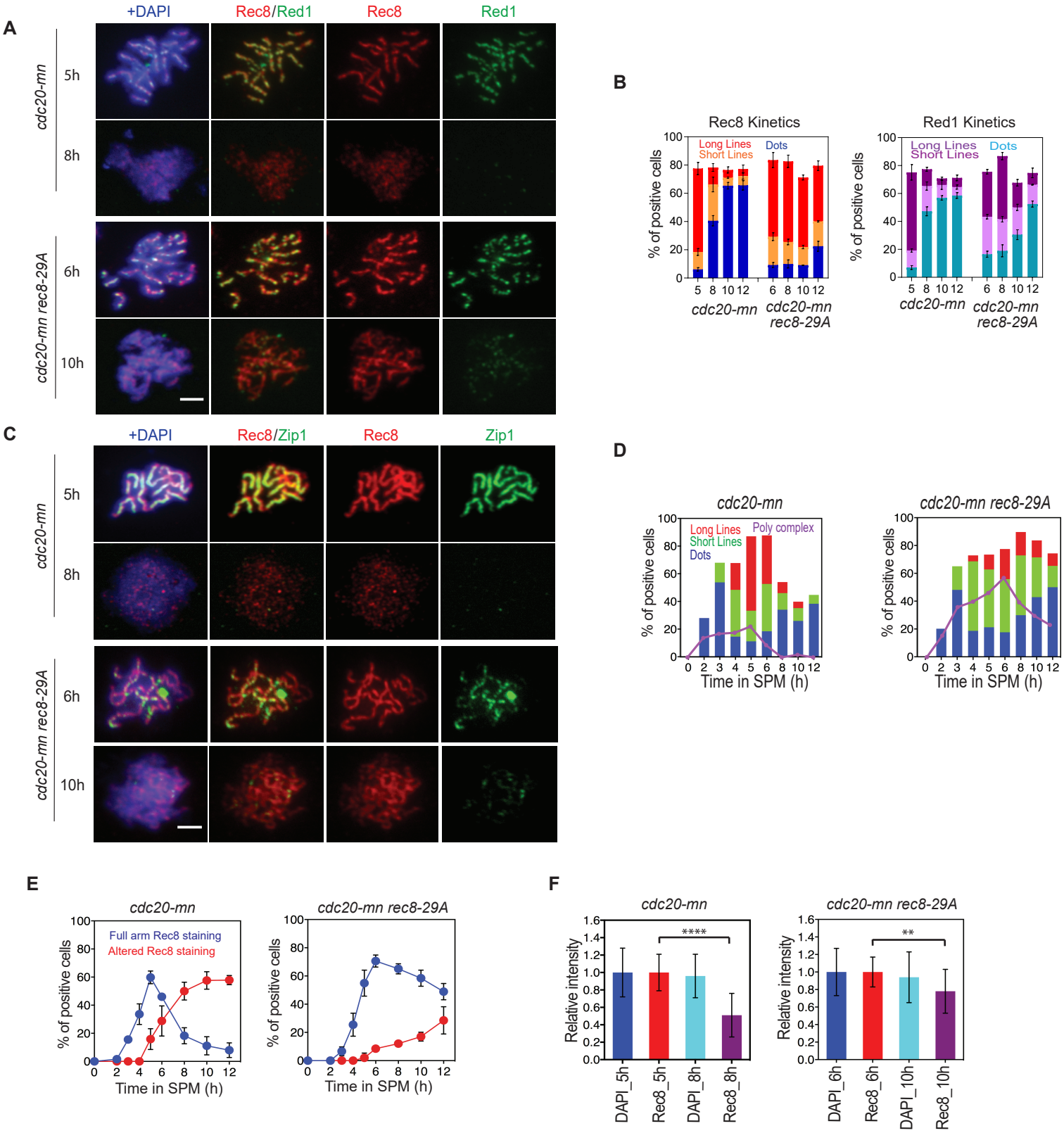

Challa et al. Figure 5

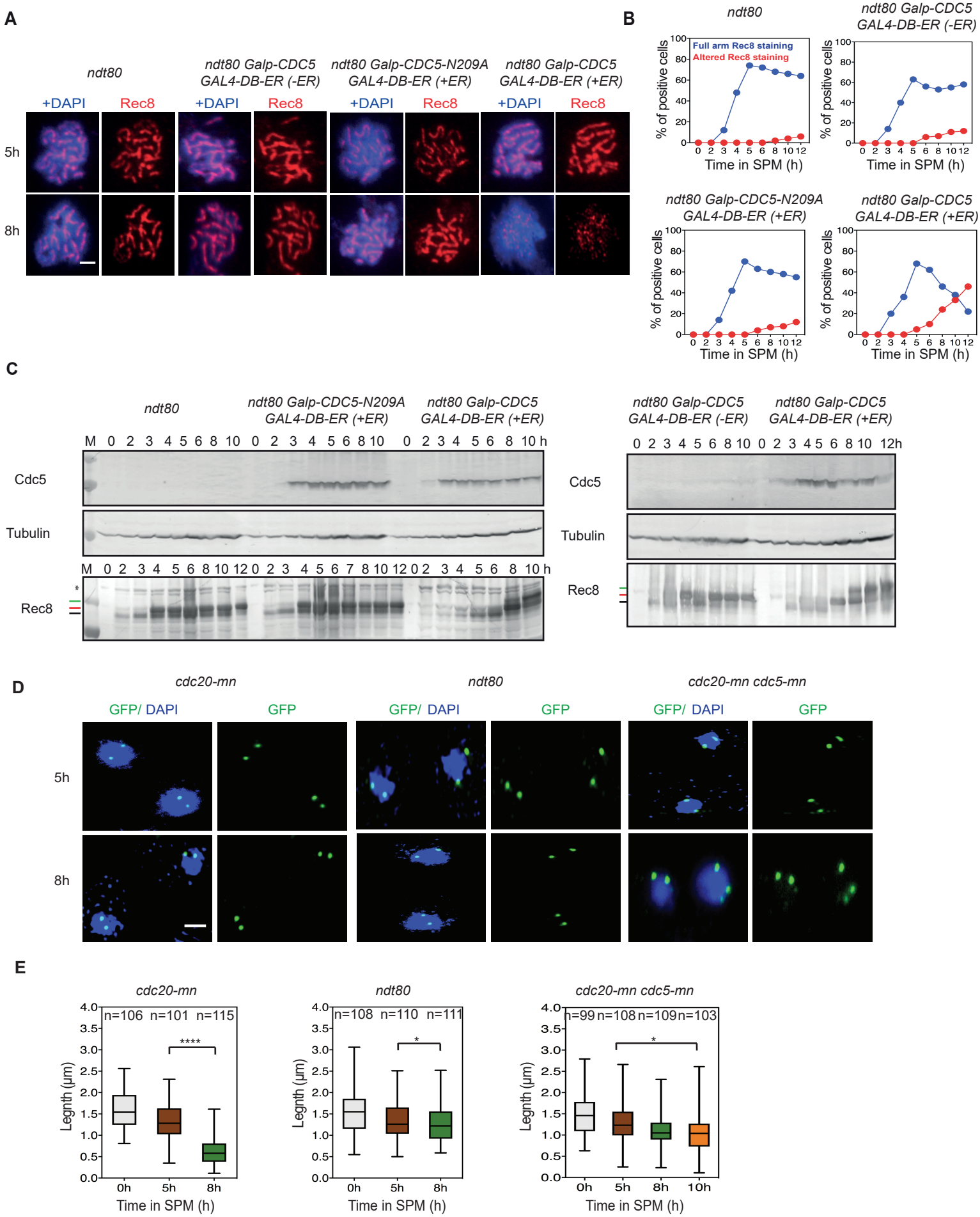

Challa et al. Figure 6

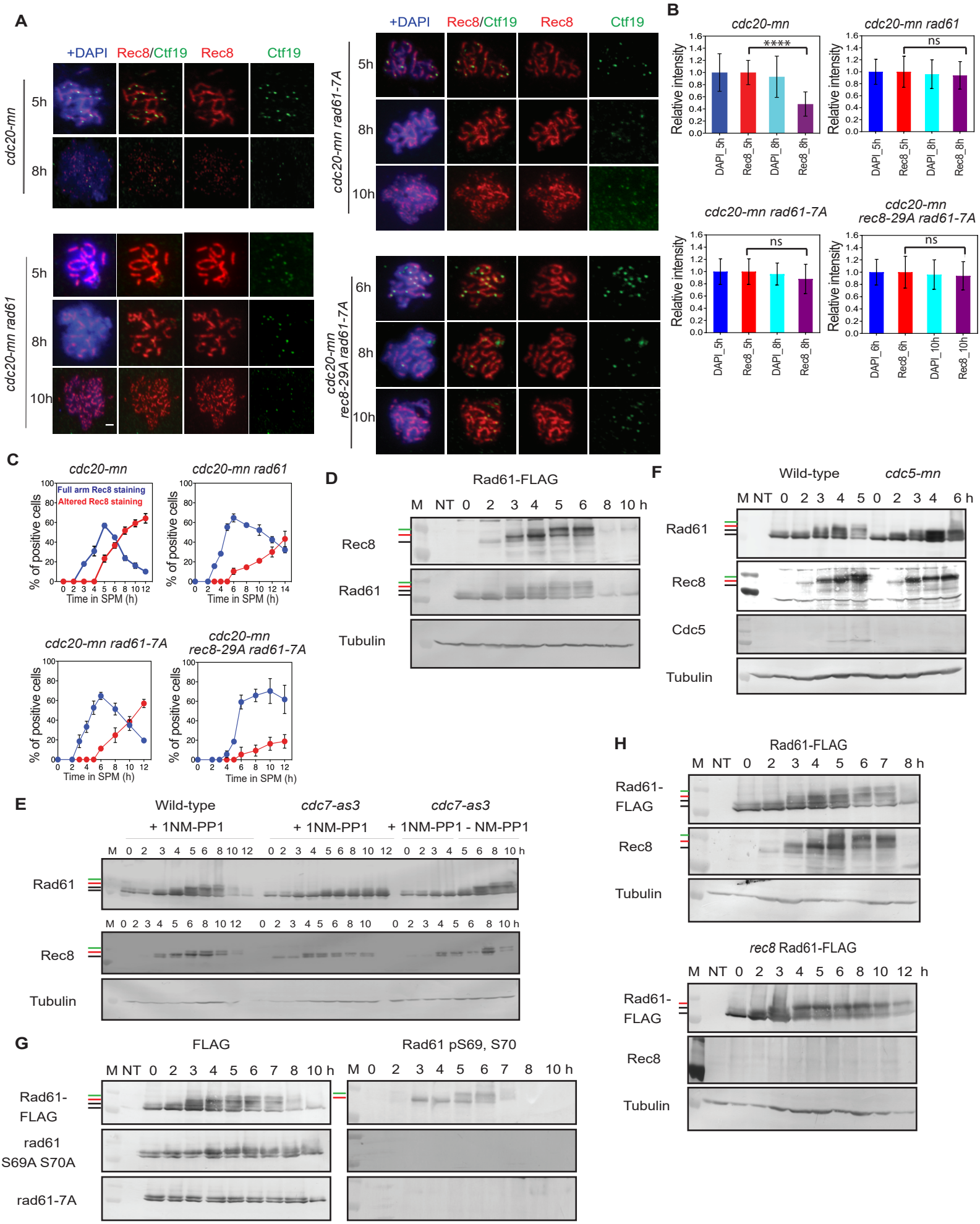
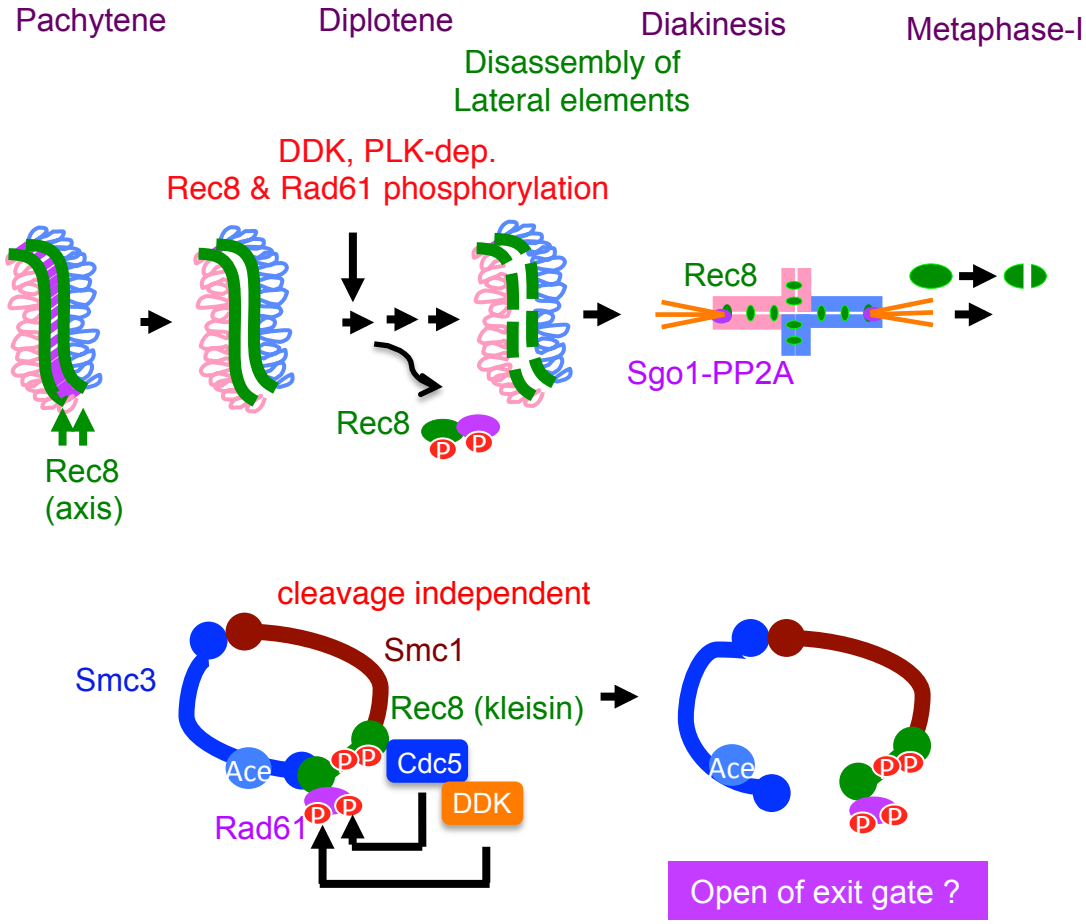
Figure 7 Challa et al.